Solution Structure of an RNA Duplex Including a C−U Base Pair[†,‡]

Yoshiyuki Tanaka,[§,||] Chojiro Kojima,[§,⊥] Toshio Yamazaki,[§] Takashi S. Kodama,[§] Kazuhiro Yasuno,[§] Shin Miyashita,[⊥] Akira (Mei) Ono,[⊥] Akira (Sho) Ono,[⊥] Masatsune Kainosho,[⊥] and Yoshimasa Kyogoku*[,§,#]

Institute for Protein Research, Osaka University, Osaka 565-0871, Japan and the Faculty of Science, Tokyo Metropolitan University, Tokyo 192-0364, Japan

Received January 5, 2000; Revised Manuscript Received March 31, 2000

ABSTRACT: The formation of the C−U base pair in a duplex was observed in solution by means of the temperature profile of ^{15}N chemical shifts, and the precise geometry of the C−U base pair was also determined by NOE-based structure calculation. From the solution structure of the RNA oligomer, r[CGACUCAGG]·r[CCUGCGUCG], it was found that a single C−U mismatch preferred being stacked in the duplex rather than being flipped-out even in solution. Moreover, it adopts an irregular geometry, where the amino nitrogen (N4) of the cytidine and keto-oxygen (O4) of the uridine are within hydrogen-bonding distance, as seen in crystals. To further prove the presence of a hydrogen bond in the C−U pair, we employed a point-labeled cytidine at the exocyclic amino nitrogen of the cytidine in the C−U pair. The temperature profile of its ^{15}N chemical shift showed a sigmoidal transition curve, indicating the presence of a hydrogen bond in the C−U pair in the duplex.

It is widely recognized that mismatches in double helical regions are important for the RNA molecules, since biologically active RNA molecules, such as ribosomal RNAs (rRNAs)[1] and transfer RNAs (tRNAs), include mismatches in the double helical regions. Nowadays, the base pairing of G−U and G−A is well-known. They form stable base pairs in duplexes. However, other less-stable mismatches have not yet been studied well. There is no clear answer for the simple question of whether these relatively unstable mismatches are stacked in a duplex or flipped out from it. In this sense, the C−U mismatch is a good candidate for studying this problem, since it is known to be one of the least stable mismatches (*1*−*4*).

The existence of a C−U mismatch in a duplex has been postulated in eucaryotic and procaryotic rRNAs (*5*, *6*), and also in tRNAs from *Schizosaccharomyces pombe*, *Mycobacterium tuberculosis*, and pea mitochondria (*7*−*9*). Then, the crystal structures of C−U pairs were determined (*10*−*12*), but there is a possibility that they are artifacts due to crystal packing. This is the reason we started to study the solution structure of a C−U mismatch. Recently, two solution structures of a C−U pair in hairpin loops were reported (*13*, *14*). Interestingly, their arrangements converged to different structures for the same loop sequences under slightly different conditions. Therefore, without proof of the presence of hydrogen bonding, the arrangement of the C−U pair in solution cannot be concluded confidently. In contrast, ^{15}N NMR spectroscopy, such as ^{15}N−^{15}N scalar coupling (*15*) and a temperature profile of ^{15}N chemical shift (*16*−*20*), provides a model-independent insight into local hydrogen bonding and the arrangement of a base pair. Although the direct measurement of the ^{15}N−^{15}N scalar coupling provides a strong evidence for hydrogen bonding, its application is limited to the case where an acceptor of hydrogen bonding is nitrogen, whereas the ^{15}N chemical shift of the donor group is measurable for all types of hydrogen bonding acceptors.

In this study, we synthesized a double-stranded RNA oligomer, rCU9 (r[CGACUCAGG]·r[CCUG(^{15}N4)CGUCG]). An ^{15}N-labeled cytidine at an exocyclic amino nitrogen was incorporated. Then we determined the solution structure of rCU9 by means of NOE-based structure calculations to reveal the global structure of rCU9 as well as the arrangement of the C−U pair. To prove the presence of the hydrogen bond in the C−U pair, we monitored ^{15}N NMR chemical shift changes versus temperature.

MATERIALS AND METHODS

Sample Preparation. Cytidine 3′-phosphoramidite labeled at the exocyclic amino group with ^{15}N was synthesized as described (*21*). Then it was introduced to the oligomer by the solid-phase phosphoramidite method with a DNA synthesizer, model 380B or 394 (ABI). The oligomers used for experiments are listed below. The ^{15}N-labeled cytidine

[†] This work was supported by a Grant-in-Aid for Basic Scientific Research, Category B (No. 09480176), from the Ministry of Education, Science and Culture, Japan, and the Human Frontier Science Program.

[‡] Protein Data Bank entry: 1C4L.

* To whom correspondence should be addressed. Phone: 81-6-6879-8597. Fax: 81-6-6879-8599. E-mail: kyogoku@protein.osaka-u.ac.jp.

[§] Division of Molecular Biophysics, Institute for Protein Research, Osaka University, 3-2 Yamadaoka, Suita, Osaka 565-0871, Japan.

[⊥] Faculty of Science, Tokyo Metropolitan University, Hachioji, Tokyo 192-0364, Japan.

[||] Present address: National Institute for Advanced Interdisciplinary Research, 1-1-4 Higashi, Tsukuba, Ibaraki 305-8562, Japan.

[#] Present address: Department of Applied Physics and Chemistry, Fukui Institute of Technology, 3-6-1 Gakuen, Fukui, 910-8505, Japan.

[1] Abbreviations: ms, millisecond; *E. coli*, *Escherichia coli*; rRNA, ribosomal RNA; tRNA, transfer RNA; DSS, 2,2-dimethyl-2-silapentane-5-sulfonate; NMR, nuclear magnetic resonance; NOE, nuclear Overhauser effect.

10.1021/bi000018m CCC: $19.00
Published on Web 05/26/2000

Scheme 1

at the exocyclic amino group is presented as (^{15}N4)C.

r[CCUG(^{15}N4)CGUCG] (rC9)

r[CGACUCAGG] (rU9)

r[CGACGCAGG] (rG9)

r[CGACUCAGG]·r[CCUG(^{15}N4)CGUCG] (rCU9)

r[CGACGCAGG]·r[CCUG(^{15}N4)CGUCG] (rCG9)

rCU9 and rCG9 are numbered sequentially from left (C1) to right (G9) (Scheme 1). The synthesized oligomers were purified as described (*22*, *23*) and quantitated as to the UV absorbance at 260 nm after nuclease P1 digestion.

NMR Measurement. The solutions for NMR measurements comprised 2 mM duplex oligomer, 20 mM sodium phosphate buffer, pH 7.0, and 50 mM NaCl in 90% H_2O/10% D_2O or 100% D_2O.

For the assignment of amino proton resonances of the cytidine in the C−U pair, an ^{1}H-^{15}N HSQC spectrum was measured (Figure 1A). Two correlation peaks between two amino protons and an amino nitrogen were observed in the ^{1}H-^{15}N HSQC spectrum, and NOE cross-peaks between two amino protons were also observed in the NOESY spectrum in Figure 1B. The amino proton resonances of the C−U pair, which appeared at different positions from other amino proton resonances for the Watson−Crick base pairs, were definitely assigned.

The assignment of other proton resonances was carried out as described (*24*). Prior to sequential NOE walks, the intraresidue cross-peaks of H5 and H6 were identified using COSY spectra. Sequential NOEs between anomeric protons and base protons of H6/H8 were followed completely through the sequences of both strands (Figure S1, Supporting Information) as well as those between sugar protons (H2′ and H3′) and base protons (Figure S2, Supporting Information). To resolve severe signal overlaps, NOESY spectra with a short mixing time of 50 ms were measured extensively at different temperatures. It was efficient to use these spectra for confirmation of the assignments of H2′ resonances since intraresidue cross-peaks between H1′ and H2′ always give strong cross-peaks at any temperature. H4′ resonances were also assigned using intraresidue cross-peaks with H1′ protons in the NOESY spectrum (Figure S3, Supporting Information). Then, residual cross-peaks between the sugar protons and the base protons were assigned to H5′ or H5″. The assignments of sugar protons derived from NOESY spectra may not be certain. To confirm the assignments, the following experiments were performed. ^{1}H-^{31}P HETCOR (*25*) gave all the ^{31}P−H3′ connectivities and part of ^{31}P−H5′ or ^{31}P−H5″. Two-quantum correlation spectroscopy gave all the spin systems between H3′ and H4′. Finally, a natural abundance ^{1}H-^{13}C HSQC spectrum gave all the H5′ or H5″ resonances. Consequently, all the nonexchangeable protons were unambiguously assigned. Exchangeable proton resonances which were observed in the NOESY spectrum were also assigned unambiguously based on the NOE connectivities as described (*24*, *26*). Eight imino proton resonances, which corresponds to the number of expected Watson−Crick base pairs, were observed. These imino protons generated cross-peaks with amino protons and H2 of paired nucleotides, which indicates that rCU9 forms a duplex with the expected arrangement of base pairing. We also assigned 10 2′-hydroxyl protons using the TOCSY spectrum in combination with the NOESY spectrum in H_2O (*27*). The proton resonance assignments are listed in Table S1 (Supporting Information).

The NOESY spectra used for the structure calculations were measured with 1024 × 512 real points for the spectral width of 14 367.82 × 12 002.66 Hz, 16 scans for each column point, and a mixing time of 200 ms at 0 and 30 °C with a 600 MHz NMR spectrometer, Bruker DRX600. In NOESY spectra in H_2O, the sequence of WATERGATE was employed for water signal suppression (*28*).

1D-^{15}N spectra were measured at higher resolution than 0.25 ppm/point with a 500 MHz NMR spectrometer, Bruker ARX500 or DMX500, from 0 to 82 °C. The temperature of the spectrometer was calibrated using the Bruker standard temperature calibration solution according to a calibration table. The proton chemical shifts were determined relative to the external standard of 2,2-dimethyl-2-silapentane-5-sulfonate (DSS). The chemical shift of nitrogen was determined using the gyromagnetic ratios and its temperature dependency (*29*).

NOE-Based Structure Calculation. Peak picking and the measurement of peak intensities in the NOESY spectra were performed with the program, NMRPipe/PIPP system (*30*, *31*). The intensities of the cross-peaks were classified into three groups according to their peak intensities, strong, medium, and weak, using the H5−H6 cross-peak intensity as an internal standard (*32*). The upper limit of the distance constraint for each category is listed in Table 1. The peaks in the weak category could arise from spin diffusion, and its upper limit of the distance constraint was set as 6.0 Å (longer than 5.0 Å) (*32*). Finally, 433 distance constraints were used for the structure calculations. Distance and planarity constraints for Watson−Crick base pairs were also included (Table 1), since internucleotide and interstrand NOEs expected for a Watson−Crick base-paired duplex were observed as described (*26*). For the C−U pair, no constraint for base pairing was introduced. As is expected for A-form RNA duplex, rCU9 also showed canonical features of A-form RNA duplexes as follows. Significantly strong sequential NOE between H2′(i−1)-H6/H8(i) were observed through the sequence (Figure S2, Supporting Information), and most of H1′−H2′ cross-peaks were not observed in the COSY spectrum except for those of G9, C17, and G18 (data not shown), which means that the sugar puckering of the most of nucleotides except for those of G9, C17, and G18 are in

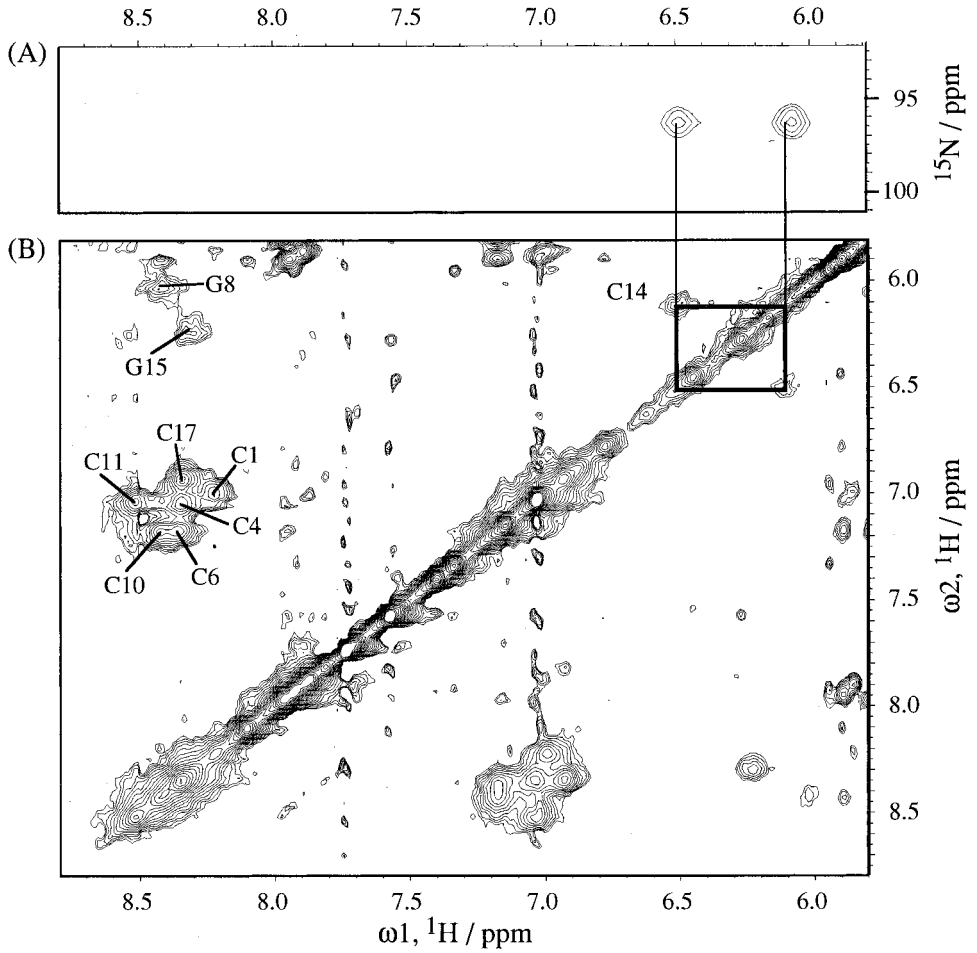

FIGURE 1: Assignment of the amino protons of the cytidine in the C−U pair. (A) ^{1}H-^{15}N HSQC spectrum (512 × 20 real points for the spectral width of 4006.4 × 709.56 Hz, at 0 °C, with a Bruker DMX500), and (B) NOESY spectrum (1024 × 512 real points for the spectral width of 14 367.82 × 12002.66 Hz, at 0 °C, with a Bruker DRX600) of the amino proton region. The cross-peaks between the two amino protons in the C−U pair are connected by bold lines. Their signals in both spectra are connected by thin lines. Cross-peaks of the amino protons in guanosines and cytidines in the C−G pair are also presented. However, those of G2, G9, G13, and G18 were not observed. Those for adenosines are too broad to be observed at this threshold.

Table 1: Statistics of Constraints and Calculated Structures

no. of the NOEs	
total	433
NOEs/residue	24.1
upper limit of the distance constraints	
strong	3.5 Å
medium	4.5 Å
weak	6.0 Å
empirical restraints for the Watson−Crick base pairing (except for the C−U pair)	
hydrogen-bonding distance	54
planarity	8 base pairs
dihedral angle restraints	
C3′-endo sugar puckering	15 residues except for G9, C17, and G18
violations of NOEs > 0.4 Å	none
deviations from standard values (heavy atoms)	
bond	0.0053 ± 0.000 04
angle	1.5 ± 0.02
improper	0.40 ± 0.009
avg rmsd from mean structure	
all heavy atom	0.72 Å

C3′-endo. Accordingly, weak restraints of C3′-endo puckering was also introduced in the refinement step except for those of G9, C17, and G18 (Table 1).

Structure calculations were performed by means of simulated annealing following guidelines reported (*32*) with minor modifications. Randomized initial structures were generated by means of molecular dynamics at 350 K without experimental constraints. Then they were used for simulated annealing. Forty-seven roughly folded structures were derived from 50 cycles of simulated annealing. Finally, 18 structures which satisfied a covalent geometry and experimental constraints were derived after the refinement of the 47 structures following the rejection criterion (*32*). All structure calculations were performed with X-PLOR ver. 3.8.1 or 3.851 (*33*). The statistics for the final structures are listed in Table 1. QUANTA 96 at Research Center for Structural Biology was used for graphics. The atomic coordinates have been deposited with Protein Data Bank (PDB code 1C4L).

RESULTS

NOE-Based Structure Calculation. The structures were calculated by simulated annealing with NOE constraints and base-pairing constraints for regular base pairs (Table 1). The resulting 47 roughly folded structures obtained on 50 times repeated simulated annealing were subjected to refinement. Finally, 18 structures which satisfied the covalent geometry and distance constraints most were accepted following the guidelines reported (*32*). We emphasize that no base-pairing constraints were applied to the C−U pair during the

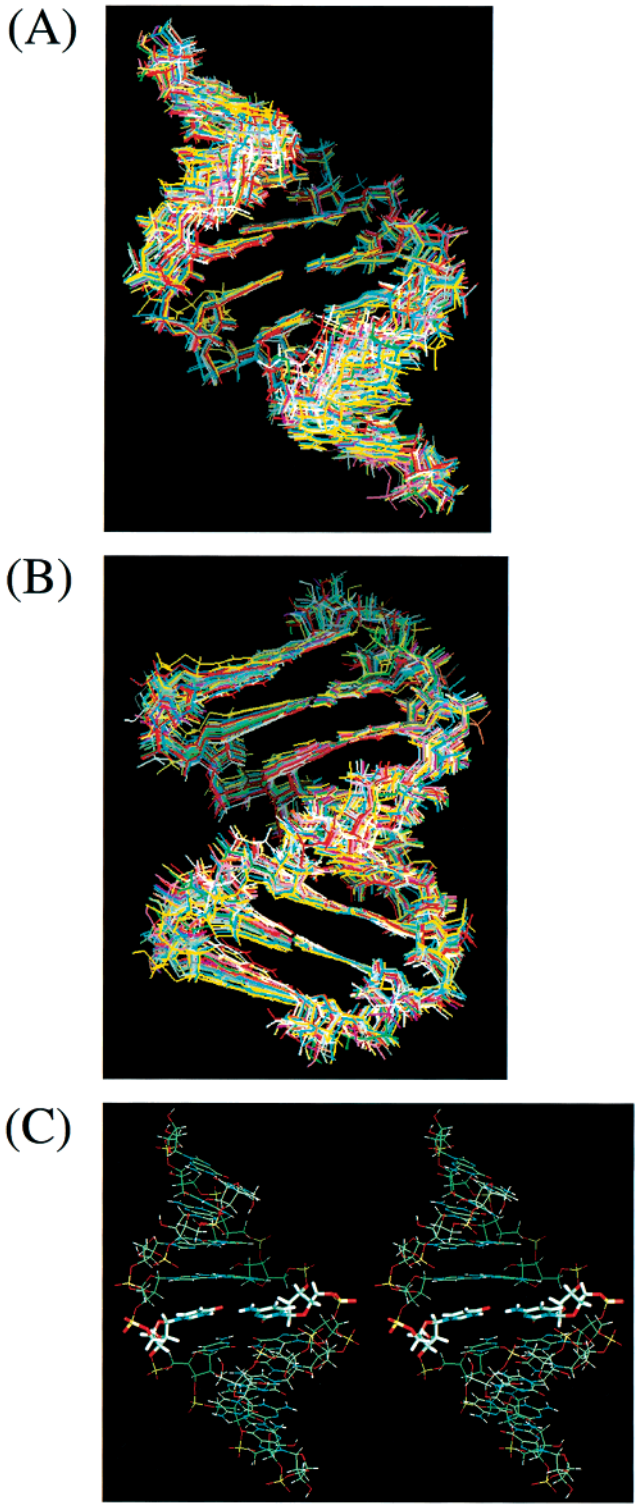

FIGURE 2: Superposition of the 18 calculated solution structures of rCU9. (A) View from the major groove. (B) Side view. (C) A stereodiagram of average structure of rCU9.

calculations, and two independent extended single strands of rC9 and rU9 were randomized by means of the molecular dynamics at 350 K without experimental constraints to generate truly random initial structures for simulated annealing. The superpositions of the 18 calculated structures of rCU9 are presented in Figure 2, panels A and B. The average structure is also presented in Figure 2C with the C−U pair highlighted. The statistics for the final structures are listed in Table 1. All of the 18 structures converged to a right-handed double helical structure with the C−U mismatch stacked in the duplex (Figure 2). It was found that the C−U mismatch preferred being stacked in a duplex to being flipped out.

In Figure 3, the superposition of the C−U pair in rCU9 and the crystal structure of the C−U pair in r(UGAGCU-UCGGCUC)$_2$ (*12*) are presented. As is apparent from Figure 3, the solution structure of the C−U pair was converged to quite a similar arrangement to that in crystals, where the amino nitrogen (N4) of C14 and the keto-oxygen (O4) of U5 are located within hydrogen bonding distance (3.0 ± 0.10 Å).

Then we further compared the structure with that found in crystals in detail. The crystal and solution structures of the C−U pair resemble each other (0.37 Å in rmsd for base moieties). The characteristic structural features of the C−U pair in the crystals presented in Figure 3B are also kept in solution, such as the C1′(cytidine)−C1′(uridine) distance, the hydrogen bonding related angles of C4(C14)−N4(C14)−O4(U5) and C4(U5)−O4(U5)−N4(C14), and the anti-conformations of χ angles of cytidine and uridine. NOE-based structure calculation indicated that a single C−U mismatch also forms a base pair and its arrangement is the same as that found in crystals (*10*−*12*).

In our structures, the amino group of C14 acts as a hydrogen-bonding donor, and O4 of U5 as a hydrogen-bonding acceptor. This arrangement is the same as that found in the C−U pair in the HDV ribozyme central hairpin loop region (*14*), but different from that found in the same loop sequence (*13*), where the hydrogen bonding acceptor is not O4 but O2 of uridine. Although C−U pairs have already been observed in solution, there is a large difference between the C−U pairs in rCU9 and the HDV ribozyme central hairpin loop region. The C−U pair in the HDV ribozyme central hairpin loop region is located in the initiation site of the loop region and there is great flexibility around the C−U pair, whereas that in rCU9 is sandwiched between two Watson−Crick base pairs and is restricted to a small conformational space. Therefore, it was not clear whether a cytidine and an uridine in a single C−U mismatch could favorably interact with each other. Nevertheless, a single C−U mismatch in a duplex also forms a C−U pair in the same arrangement as those found in the internal and hairpin loop regions (*10*−*12*, *14*).

Temperature Profile of the Amino Nitrogen Chemical Shift. The arrangement of the C−U pair in solution was found to be the same as that in crystals. It is still unclear whether the geometry of the C−U pair in Figure 3A is due to a hydrogen bond between the amino group of C14 and the keto-oxygen (O4) of U5 or just a result of stacking interaction between neighboring Watson−Crick base pairs. Until the presence of a hydrogen bond is directly proven, the C−U pair cannot be regarded as a real base pair. To confirm the presence of this hydrogen bond, we monitored the temperature-dependent chemical shift changes of ^{15}N-nucleus at the exocyclic amino group of the C−U pair. (Since the hydrogen bond acceptor in the C−U pair is oxygen not nitrogen, ^{15}N−^{15}N scalar coupling cannot be observed for the C−U pair.) The chemical shift of a nitrogen atom is very sensitive to the hydrogen bond, and those in nucleic acids have been studied by Jones' group (*16*−*20*). According to their data, breakage of the hydrogen bond gives an upfield-shift of the ^{15}N

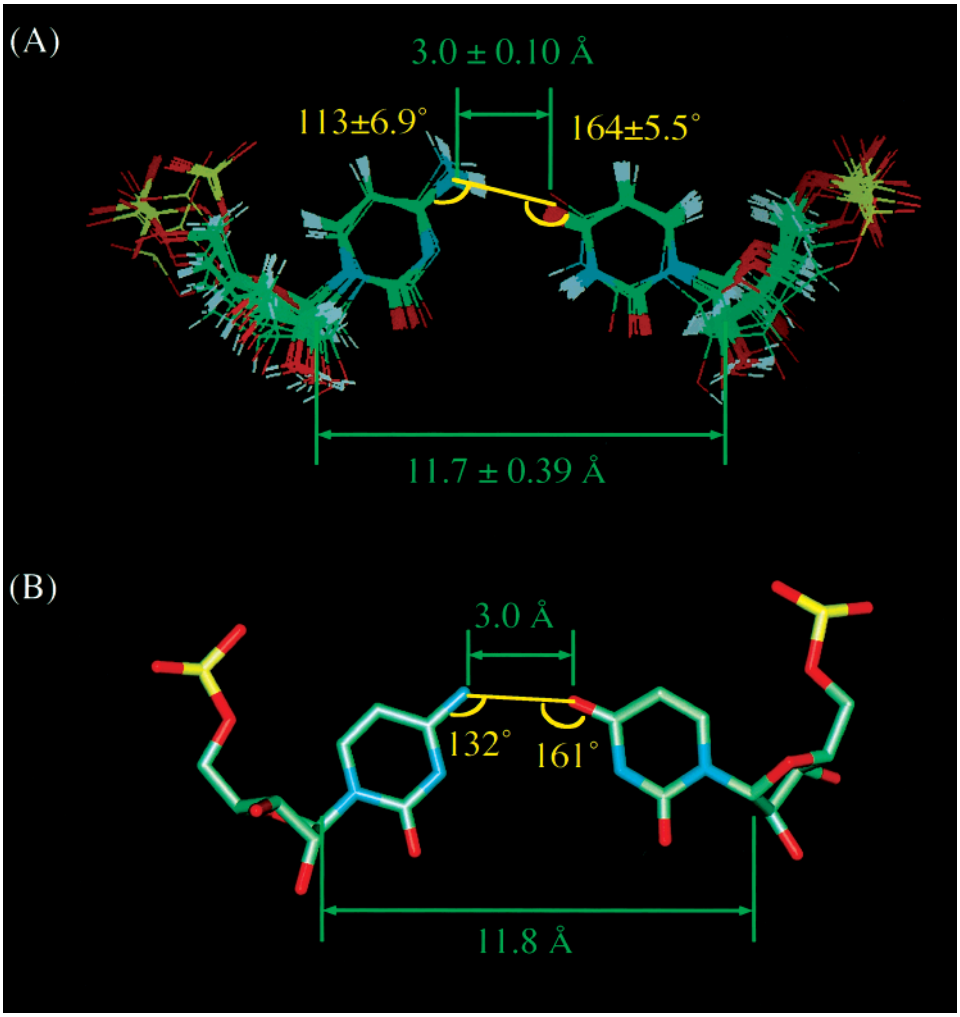

FIGURE 3: (A) Superposition of the C−U pair in solution. Least-squares fitting was performed using base moieties of the C−U pair. (B) Crystal structure of the C−U pair in r(UGAGCUUCGGCUC) (*12*). Characteristic distances and angles in the crystal structure are also presented in the figure. In the case of the solution structures, the average values and their standard deviations are indicated.

chemical shift of the exocyclic amino group by raising the temperature. Then, we measured 1D-^{15}N spectra of the amino nitrogens in rCU9, rCG9, rC9, and the cytidine monomer at different temperatures for the samples. The resulting temperature profiles are presented in Figure 4. The chemical shifts of rCG9 are an example of the case when the amino nitrogen is incorporated in a strong hydrogen bond of a Watson−Crick C−G base pair, while those of rC9 and the cytidine monomer are examples without hydrogen bond interaction. The temperature profile of the amino nitrogen in the C−U pair, which is indicated by circles (rCU9), showed sigmoidal transition upfield (Figure 4), which demonstrates the presence of the hydrogen bond. This transition is evidence of the presence of a hydrogen bond in the C−U pair. The ^{15}N-chemical shift value for rCU9 falls between those of rC9 and rCG9 at lower temperatures. This may indicate that the amino group of cytidine forms a hydrogen bond in the C−U pair, but it is weaker than that in a Watson−Crick C−G pair.

It is known that the atom groups hydrogen bonded to a carbonyl oxygen tend to be oriented in the direction of the lone pair of a carbonyl oxygen in crystals (*34*, *35*). All the hydrogen-bond-related angles in Watson−Crick base pairs, such as C6(G)−O6(G)−N4(C) and C4(U)−O4(U)−N6(A), are oriented in the direction of the lone pair (approximately 120°). In contrast, the angle of C4(U5)−O4(U5)−N4(C14) (164 ± 5.5°) (Figure 3) is deviated from it. This is consistent with the fact that the hydrogen bond in the C−U pair is weak.

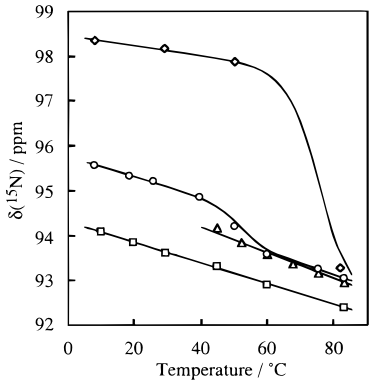

FIGURE 4: Temperature profiles of the chemical shifts of cytidine amino groups. Diamonds, circles, triangles and rectangles represent rCG9, rCU9, rC9, and the cytidine monomer, respectively. The oligomer, rC9, forms an unstable self-associated duplex at temperatures lower than 40 °C, and signals were not observed. Therefore, the chemical shift values below 40 °C are not plotted. In the case of rCG9, it melts above 50 °C, and signals were not observed during the transition. Therefore, putative temperature profile, generated from thermodynamic parameter of rCG9 (ΔH of −350 kJ mol^{-1} and ΔS of −950 JK^{-1}mol^{-1}), is presented. Whereas, rCU9 melts arround 45 °C.

DISCUSSION

We revealed the arrangement of a C−U pair in solution by means of NOE-based structure calculation. In crystals, the location of the C−U pair significantly shifted toward a minor groove by 2 Å (*10*−*12*, *36*). In the calculated solution structure, the C−U pair also shifted toward the minor groove compared with a Watson−Crick base pair and was sandwiched between neighboring base pairs. The C−U pair is thought to be stabilized by not only a direct hydrogen bond between paired nucleotides but also their stacking with neighboring Watson−Crick base pairs. In addition, the observation of 2′-hydroxyl protons of C4 and G13 as well as some other residues may suggest the presence of hydrogen-bonding interactions to neighboring residues, since 2′-hydroxyl protons are rarely observed for mononucleotides (*27*). Then, we calculated the average distances between O2′ at a residue and O4′ at the 3′-neighboring residue (O2′−O4′ distances) for 16 possible sites among 18 calculated structures, and found that 14 O2′−O4′ distances were within a hydrogen bonding distance. These results are consistent with highly cooperative dissociation of the C−U pair with that of other Watson−Crick base pairs in rCU9. Thermal denaturation experiments on rCU9 with circular dichroism (CD) spectra showed a canonical single transition, and the plot of T_m versus the concentration of rCU9 also suggested a two-state equilibrium of rCU9 (*36*). It was found that an oligomer including a single C−U mismatch is stable enough to maintain a duplex but it becomes more stable when the C−U pair is replaced by a Watson−Crick C−G pair. By means of thermal denaturation experiments with CD spectra, the T_m value of the duplex rCG9 is higher by approximately 20 °C than that of rCU9 at the same concentration (rCU9, ΔH of −375 kJ mol^{-1} and ΔS of −1101 J K^{-1}mol^{-1}; rCG9, ΔH of −350 kJ mol^{-1} and ΔS of −950 JK^{-1}mol^{-1} for solution containing 50 mM NaCl) (T.S. Kodama, unpublished data).

We obtained the evidence of the presence of hydrogen bonding in the C−U base pair from the temperature profile of ^{15}N chemical shifts. Without this result, we could not confidently determine the arrangement of the C−U base pair by means of NOE-based structure calculation, since there existed one exceptional structure in the 18 calculated structures. The bases of the C−U mismatch were out of hydrogen bonding distance (3.35 Å for the distance between the amino nitrogen of C14 and the keto-oxygen of U5). Similarly, in the solution structure of the hairpin loop region in HDV ribozymes (*13*, *14*), large dispersion was observed between converged structure. To determine the arrangement of a novel base pair, ^{15}N NMR chemical shift is employed as it reveals local hydrogen bonding. ^{15}N NMR chemical shifts can be monitored for uniformly labeled samples as well as a point-labeled ones.

As mentioned in the introductory portion of this paper, ^{15}N NMR spectroscopy can provide model-independent insight into local hydrogen bonding, such as ^{15}N−^{15}N scalar coupling (*15*) and temperature profile of ^{15}N-chemical shift (*16*−*20*). However, ^{15}N−^{15}N scalar coupling was not applicable to the C−U pair, since hydrogen bonding in the C−U pair is formed between the amino group and the keto-oxygen atom (NH−O type). Therefore, we monitored temperature profile of ^{15}N NMR chemical shift, instead. The temperature profile of the amino nitrogen in the C−U pair showed sigmoidal transition curve from downfield to upfield (Figure 4) like a temperature profile of UV absorbance, which indicates the presence of hydrogen bonding. More interestingly, the method of the temperature profile gave us information about weak hydrogen bonding such as that in the C−U pair. Although the method of ^{15}N-^{15}N scalar coupling provides more direct evidence for hydrogen bonding, that of the temperature profile is still valuable. These two methods are complimentary with each other.

All the results presented here suggest that the C−U pair in RNA molecules does not disrupt the formation of a duplex or interrupt the continuity of a double helix either. This is an important point for the prediction of the secondary and tertiary structures of larger RNA molecules. In many cases of secondary structure predictions, C−U mismatches are assigned to the loop, as seen in the case of the putative hairpin loop region in HDV ribozyme. However, a C−U mismatch in the loop beginning site forms a base pair (*13*, *14*). These results suggest that a C−U mismatch prefers to form a base pair. In a DNA duplex, a C−T mismatch which is an analogous mismatch to C−U in DNA also showed a stacked conformation (*37*). These data together with our data indicate that the treatment of a C−U mismatch in secondary structure prediction should be reinvestigated. From these data, we can speculate that putative single C−U mismatches in rRNAs (*5*, *6*), and in tRNAs from *Schizosaccharomyces pombe*, *Mycobacterium tuberculosis*, and pea mitochondria (*7*−*9*) could form base pairs.

We determined the three-dimensional solution structure of an RNA duplex including a single C−U mismatch and also revealed that a single C−U mismatch in a duplex surely forms a base pair with a hydrogen bond in the arrangement as seen in crystals (*10*−*12*). It is reasonably safe to conclude that ^{15}N NMR chemical shifts should be monitored combined with NOE-based structure calculation to determine the arrangements of unknown non-Watson−Crick base pairs in solution.

ACKNOWLEDGMENT

The authors wish to thank Dr. Yasuo Komatsu, Hokkaido University, for the procedure of an RNA purification. The authors also wish to thank Dr. Hiromu Sugeta, Osaka University, for programming of the least-squares calculation for thermodynamic analysis, and Dr. Koichi Uegaki at ONRI for helpful comments.

SUPPORTING INFORMATION AVAILABLE

One chemical shift table and three figures of the 2D-NOESY spectra for anomeric protons (H1′)−base protons (H8, H6) cross section, base protons (H8, H6)−sugar protons (H2′, H3′, H4′, H5′, H5″) cross section, and anomeric protons (H1′)−sugar protons (H2′, H3′, H4′, H5′, H5″) cross section. This material is available free of charge via the Internet at http://pubs.acs.org.

REFERENCES

1. SantaLucia, J., Jr., Kierzek, R., and Turner, D. H. (1991) *Biochemistry 30*, 8241−8251.
2. He, L., Kierzek, R., SantaLucia, J., Jr., Walter, A. E., and Turner, D. H. (1991) *Biochemistry 30*, 11124−11132.

3. Wu, M., McDowell, J. A., and Turner D. H. (1995) *Biochemistry 34*, 3204−3211.
4. Zhu, J., and Wartell, R. M. (1997) *Biochemistry 36*, 15326−15335.
5. Gutell, R. R., Larsen, N., and Woese, C. R. (1994) *Microbiol. Rev. 58*, 10−26.
6. Schnare, M. N., Damberger, S. H., Gray, M. W., and Gutell, R. R. (1996) *J. Mol. Biol. 256*, 701−719.
7. Vögeli, G. (1979) *Nucleic Acids Res. 7*, 1059−1065.
8. Vasanthakrishna, M., Kumar, N. V., and Varshney, U. (1997) *Microbiology 143*, 3591−3598.
9. Schock, I., Maréchal-Drouard, L., Marchfelder, A., and Binder, S. (1998) *Mol. Gen. Genet. 257*, 554−560.
10. Holbrook, S. R., Cheong, C., Tinoco, I., Jr., and Kim, S.-H. (1991) *Nature 353*, 579−581.
11. Cruse, W. B., Saludjian, P., Biala, E., Strazewski, P., Prangé, T., and Kennard, O. (1994) *Proc. Natl. Acad. Sci. U.S.A. 91*, 4160−4164.
12. Tanaka, Y., Fujii, S., Hiroaki, H., Sakata, T., Tanaka, T., Uesugi, S., Tomita, K.-I., and Kyogoku, Y. (1999) *Nucleic Acids Res. 27*, 949−955.
13. Kolk, M. H., Heus, H. A., and Hilbers, C. W. (1997) *EMBO J. 16*, 3685−3692.
14. Lynch, S. R., and Tinoco, I., Jr. (1998) *Nucleic Acids Res. 26*, 980−987.
15. Pervushin, K., Ono A., Fernández C., Szyperski, T., Kainosho, M., and Wütrich, K. (1998) *Proc. Natl. Acad. Sci. U.S.A. 95*, 14147−14151.
16. Gao, X., and Jones, R. A. (1987) *J. Am. Chem. Soc. 109*, 3169−3171.
17. Goswami, B., Gaffney, B. L., and Jones, R. A. (1993) *J. Am. Chem. Soc. 115*, 3832−3833.
18. Gaffney, B. L., Goswami, B., and Jones, R. A. (1993) *J. Am. Chem. Soc. 115*, 12607−12608.
19. Zhang, X., Gaffney, B. L., and Jones, R. A. (1997) *J. Am. Chem. Soc. 119*, 6432−6433.
20. Zhang, X., Gaffney, B. L., and Jones, R. A. (1998) *J. Am. Chem. Soc. 120*, 615−618.
21. Kataoka, S., Shiina, T., Ono (Mei), A., Tate, S., Ono (Sho), A., and Kainosho, M. (1996) *Nucl*eic *Acids Symp. Ser. 35*, 93−94.
22. Komatsu, Y., Koizumi, M., Sekiguchi, A., and Ohtsuka, E. (1993) *Nucleic Acids Res. 21*, 185−190.
23. Komatsu, Y., Kanzaki, I., and Ohtsuka, E. (1996) *Biochemistry 35*, 9815−9820.
24. Varani, G., and Tinoco, I., Jr. (1991) *Q. Rev. Biophys. 24*, 479−532.
25. Sklenár, V., Miyashiro, H., Zon, G., Miles, H. T., and Bax, A. (1986) *FEBS Lett. 208*, 94−98.
26. Hues, H. A., and Pardi A. (1991) *J. Am. Chem. Soc. 113*, 4360−4361.
27. Gyi, J. I., Lane, A. N., Conn, G. L., and Brown, T. (1998) *Nucleic Acids Res. 26*, 3104−3110.
28. Piotto, M., Saudek, V., and Sklenár, V. (1992) *J. Biomol. NMR 2*, 661−665.
29. Wishart, D. S., Bigam, C. G., Yao, J., Abildgaard, F., Dyson, H. J., Oldfield, E., Markley, J. L., and Sykes, B. D. (1995) *J. Biomol. NMR 6*, 135−140.
30. Garrett, D. S., Powers, R., Gronenborn, A. M., and Clore, G. M. (1991) *J. Magn. Reson. 95*, 214−220.
31. Delaglio, F., Grezesiek, S., Vuister, G. W., Zhu, G., Pfeifer, J., and Bax, A. (1995) *J. Biomol. NMR 6*, 277−293.
32. Allain, F. H.-T., and Varani, G. (1997) *J. Mol. Biol. 267*, 338−351.
33. Brünger, A. T. X-PLOR, version 3.1 manual, Yale University Press, New Haven, CT, 1992.
34. Thanki, N., Thornton, J. M., and Goodfellow, J. M. (1988) *J. Mol. Biol. 202*, 637−657.
35. Ippolito, J. A., Alexander, R. S., and Christianson, D. W. (1990) *J. Mol. Biol. 215*, 457−471.
36. Tanaka, Y. Doctoral Thesis, Graduate School of Science, Osaka University, 1998.
37. Boulard, Y., Cognet, J. A. H., and Fazakerley, G. V. (1997) *J. Mol. Biol. 268*, 331−347.

BI000018M